American Journal of Pathology, Vol. 149, No. 5, November 1996

Correlation between Enhanced Vascular Permeability, Up-Regulation of Cellular Adhesion Molecules and Monocyte Adhesion to the Endothelium in the Retina during the Development of Fatal Murine Cerebral Malaria

Naili Ma,* Nicholas H. Hunt,*
Michele C. Madigan,† and Tailoi Chan-Ling‡

From the Departments of Pathology, Clinical Ophthalmology,† and Anatomy and Histology,‡ University of Sydney, Sydney, Australia*

The relationships between increased vascular permeability to protein, monocyte adherence to the endothelium, and expression of the cell adhesion molecules, intercellular adhesion molecule-1 (ICAM-1) and vascular cell adhesion molecule-1 (VCAM-1) in the central nervous system microvasculature were studied during the progression of fatal murine cerebral malaria. CBA mice were inoculated with* Plasmodium berghei *ANKA, and changes in the retinal microvasculature were examined on days 3, 5, and 7 post-inoculation (p.i.). Evans blue dye and horseradish peroxidase (HRP) were administered intravenously to assess vascular permeability to macromolecules macroscopically and by light and electron microscopy. ICAM-1 and VCAM-1 expression were examined by immunohistochemistry. HRP leakage into the retinal parenchyma was seen macroscopically at a low level on day 3 p.i., increasing progressively at day 5 (the earliest time at which cerebral symptoms were observed) and day 7 (the day on which animals showed severe behavioral abnormalities and died). The inner retinal vascular plexus showed a slight increase in vascular permeability to intravenous Evans blue at day 3 p.i. and congestion, monocyte adherence to the endothelium, and increased vascular permeability to both Evans blue and HRP at day 7 p.i. Electron microscopic observations were consistent with these findings and also revealed disrupted tight junctions and the coating of monocytes and endothelium with HRP at day 7 p.i. Immunohistochemical staining and densitometry showed a progressive increase from day 3 to day 7 p.i. in the densities of ICAM-1 and VCAM-1 on the venular endothelium of the inner retinal vascular plexus, with the appearance of adherent ICAM-1$^+$ monocytes at the terminal stage of the disease. None of the pathological changes associated with the inner retinal plexus were seen at any stage in the outer retinal plexus. These results suggest the following sequence of events in the inner retinal vessels, particularly the venules, during the progression of fatal murine cerebral malaria: 1) a mild increase in vascular permeability at approximately day 3 p.i., 2) a progressive increase in endothelial expression of the cell adhesion molecules ICAM-1 and VCAM-1, commencing at approximately day 3 p.i., 3) monocyte adhesion to the endothelium starting at approximately day 5 p.i., and 4) frank disruption of endothelial integrity at the terminal stage (day 7 p.i.), leading to edema and hemorrhage. Similar changes in cerebral vessels may underlie the neurological complications of the disease. (Am J Pathol 1996, 149:1745–1762)

Cerebral malaria (CM) is one of the major pathological complications of *Plasmodium falciparum* infection. Approximately 1% of falciparum malaria cases

Supported by grants from the National Health and Medical Research Council of Australia (to N. H. Hunt and T. Chan-Ling), Sydney Foundation for Medical Research (to M. C. Madigan), and a University of Sydney Postgraduate Research Award (to N. Ma).

Accepted for publication July 11, 1996.

Address reprint requests to Dr. Tailoi Chan-Ling, Department of Anatomy and Histology (F13), University of Sydney, NSW 2006, Australia.

develop CM and some 20% of these die. Among the prominent histopathological features in postmortem brains of CM victims are sequestration of parasitized erythrocytes in microvessels, ring hemorrhages, and edema.[1–4]

The nature of the pathogenetic mechanisms in human CM is not clear. It has been proposed that the sequestration of parasitized erythrocytes in the cerebral microcirculation leads to obstruction of blood flow and regional anoxia,[2,5,6] although there also is substantial evidence for an immunopathological component to the disease.[7–11] As it is not possible to examine the progressive development of histopathological changes in the human central nervous system (CNS) or to carry out experimental manipulations, a number of animal models of the disease have been developed. The most useful is the fatal murine cerebral malaria (FMCM) model, namely, *P. berghei* ANKA infection in CBA mice.[12–14] These mice develop behavioral changes at approximately day 5 post-inoculation (p.i.) and progress to coma and death at approximately days 6 to 8 p.i. while parasitemias are 10 to 15%.[13–15] At the terminal stage of the disease, the CNS tissue of these mice exhibits petechial hemorrhages, edema, and vascular occlusion,[13–17] all of which are features of postmortem human CM cerebral tissue.[1–4] In FMCM, CNS microvascular occlusion is a consequence of monocyte aggregation,[16,17] and although this has been observed in human CM,[11] it is more usually reported that parasitized erythrocytes are responsible for obstruction of blood flow.[2,5]

CNS vasculopathy is intimately associated with the pathogenesis of FMCM.[12–14,16,17] We have examined the role of the CNS microvasculature in the murine system not only in the brain[13,14,18] but also in the retina.[16,17] We have shown that petechial hemorrhages, edema, and changes in microvascular permeability occur in the retina in parallel with such phenomena in the brain and that examination of the retinal microvessels in whole-mount preparations allows the detection of such pathology earlier than is possible with conventional histochemical procedures in the brain.[16,17] Furthermore, a range of techniques that reveal the nature and timing of cell-cell interactions during the pathogenesis of the disease can be applied to retinal whole-mounts. Retinal involvement, including hemorrhage, edema, and sequestration of parasitized erythrocytes, is a feature of up to 35% of human CM cases.[19–21]

FMCM appears to be immunopathological in nature because it is dependent on $CD4^+$ T cells and involves monocytes, cytokines, and possibly, reactive oxygen species.[14–18,22,23] In human CM, it is proposed that parasitized erythrocytes adhere to the endothelium of the CNS microvasculature through interactions with certain cellular adhesion molecules.[24–26] This suggests a possible link between the sequestration hypothesis and the concept of immune system involvement,[9,23] for the up-regulation of adhesion molecules on the endothelium is inducible by cytokines and is commonly involved in immune and inflammatory responses.[27] Adhesion molecules such as intercellular adhesion molecule-1 (ICAM-1), vascular cell adhesion molecule-1 (VCAM-1), E-selectin, thrombospondin, and CD36 have been shown to be capable of binding *P. falciparum*-infected erythrocytes *in vitro*, to be expressed in postmortem brain tissue, or to be present in soluble form in plasma in human CM.[24–26,28,29] It therefore is considered that they play a role in the sequestration of parasitized erythrocytes in the CNS vasculature during the cerebral complications associated with *P. falciparum* infection.

For these reasons, it was of interest to further examine parallels between human CM and FMCM by investigating whether the adherence of monocytes to the endothelium in the latter condition depends on increased expression of adhesion molecules, in an analogous way to the interaction of parasitized erythrocytes with the endothelium in human CM. We also examined, in the retina, whether the increased vascular permeability to protein and the edema seen during the progression of murine CM are temporally and spatially associated with endothelial expression of cellular adhesion molecules and monocyte adherence.

Materials and Methods

Fatal Murine Cerebral Malaria (FMCM)

Six- to eight-week-old female CBA/T6 mice (approximately 20 g body weight) were inoculated intraperitoneally with a 200-μl suspension of 10^6 red blood cells infected by *P. berghei* ANKA (PbA) in phosphate-buffered saline (PBS, pH 7.4). After removal from liquid nitrogen storage, these parasites had been maintained by weekly subinoculation from the infected blood of donor mice to normal mice of the corresponding strain and sex for several weeks. More than 95% of inoculated CBA/T6 mice infected with PbA (CBA-PbA) developed cerebral symptoms at approximately day 5 p.i., including paralysis, hemiplegia, convulsions, and coma, followed by death at approximately day 6 to day 8 p.i. associated with parasitemias typically between 10 and 15%.[13,14]

Uninfected CBA mice of the same age and sex were used as controls.

Intravascular Perfusion with Evans Blue

To examine possible differences in microvascular permeability in the retina between control CBA mice and CBA PbA-infected mice on days 3 and 7 p.i. (n = 6 in each group), 200 μl of a filtered 2% (w/v) Evans blue (Sigma E 2129) solution in PBS was injected via the tail vein. The retinal whole mounts were prepared as previously described.[30]

Intravascular Perfusion with Horseradish Peroxidase (HRP)

To further investigate the relationship between changes in microvascular permeability and endothelial cell properties in retinas during the development of FMCM, control uninfected mice (n = 4) and CBA-PbA mice on days 3 (n = 3), 5 (n = 3), and 7 (n = 6) p.i. were injected intravascularly with 20 mg/100 g body weight of grade II HRP (Boehringer-Mannheim, Mannheim, Germany) dissolved in 30 mg/ml Hartmann's solution (balanced physiological saline, pH 7.0, Baxter Healthcare Proprietary, Sydney, Australia).[31] This enzyme has been used extensively as a marker of vascular permeability to proteins. To facilitate tail vein injections with HRP, CBA-PbA and CBA control mice were kept warm on a heating pad (37°C) for 20 to 30 minutes before injection. A solution of promethazine (0.1 ml of 1% (w/v) promethazine in distilled water/100 g body weight) was administered intraperitoneally to prevent an allergic reaction to HRP. After the HRP had circulated for 15 minutes, the animals were terminally anesthetized with ether. Immediately after this, the mice were perfused intracardially with 10 ml of ice-cold Hartmann's solution, followed by 10 ml of ice-cold fixative (2.5% (v/v) glutaraldehyde in 0.1 mol/L sodium cacodylate buffer (pH 7.2), containing 2 mmol/L calcium chloride and 3.4% (w/v) sucrose). Perfusion pressure was kept low to minimize damage to vessels. After perfusion, the eye cups were removed and post-fixed for 30 minutes in ice-cold fixative. Finally, the retinas were dissected as previously described[30] and fixed for an additional 30 minutes at room temperature.[31]

HRP Histochemistry for Electron Microscopy

To enhance HRP visualization, the eye cups were rinsed in cacodylate buffer (pH 7.2) for at least 1 hour after fixation and incubated for 30 minutes in cacodylate buffer containing 1 mg/ml 3,3′-diaminobenzidine (Sigma, St. Louis, MO) and then transferred to 10 ml of fresh cacodylate buffer and diaminobenzidine solution containing 0.1 ml of 3% (v/v) hydrogen peroxide to generate the colored HRP reaction product. After 5 to 10 minutes of incubation, the eye cups were rinsed in cacodylate buffer to stop the HRP reaction. They were then photographed with a dissecting microscope or prepared for electron microscopy as described below.

Electron Microscopy

Retinas were dissected into smaller pieces, post-fixed in 2% (w/v) osmium tetroxide (OsO_4) for 1 hour at room temperature, and rinsed in 2% (w/v) sodium acetate. To enable better identification of the HRP reaction product, *en bloc* staining with 2% (w/v) uranyl acetate was omitted. Tissue was then dehydrated through a graded series of alcohols and acetone and embedded in epon-araldite resin (Probing & Structure Pty., Brisbane, Australia). Semi-thin (0.5 μm) sections were mounted on glass slides, stained with 1% (w/v) toluidine blue, and examined with a light microscope. Ultrathin (50 to 70 nm) sections were collected on grids and stained with 4% (w/v) uranyl acetate and Reynold's lead citrate. Unstained sections were also assessed. Grids were examined with a Hitachi H500 transmission electron microscope at 100 kV.

Monoclonal Antibody Preparation

Rat anti-mouse ICAM-1 (YN1/1) monoclonal antibody (rat IgG_{2a}) was isolated as previously described by others.[32,33] Briefly, the antibody was subjected to ammonium sulfate precipitation from the culture supernatant and then dialyzed against PBS.[33] It was further purified by application to an immobilized protein A/G AffinityPak column (ImmunoPure (A/G) IgG purification kit 44902, Pierce). The purity of the antibody was checked by polyacrylamide gel electrophoresis and its concentration assessed spectrophotometrically at A_{280}. Finally, the purified anti-ICAM-1 antibody (concentration, 0.8 mg/ml) was sterile filtered and stored at 4°C. Rat anti-mouse VCAM-1 (429 MVCAM.A, 0.5 mg/ml) monoclonal antibody (rat IgG_{2a}) was obtained commercially (PharMingen, Australia).

Immunohistochemistry of ICAM-1 and VCAM-1

Normal CBA mice (n = 8) and CBA PbA-infected mice on days 3 (n = 8), 5 (n = 8), and 7 (n = 10) p.i. were examined. Animals were lightly anesthetized with ether and then killed by cervical dislocation. The eyes were removed and immersion fixed in 0.5% paraformaldehyde in 0.1 mol/L phosphate buffer (PBS, pH 7.4) for 30 minutes. The intact retinas were dissected out under a surgical microscope as previously described[30] and fixed in 70% ethanol at −20°C for an additional 30 minutes.

Retinas were washed in 0.1 mol/L PBS with 0.1% (v/v) Triton X-100 (pH 7.4) for 30 minutes and then incubated with either anti-ICAM-1 (1:100 diluted in 0.1 mol/L PBS with 1% (w/v) bovine serum albumin) or anti-VCAM-1 (1:50 diluted in the same solution as above) for 12 hours at 4°C. After washing, the retinas were further incubated with a biotinylated anti-rat Ig (1:50, Amersham) for 2 hours at room temperature. Retinas were then incubated with streptavidin-HRP (1:100, Amersham) for 2 hours at room temperature. Omission of the primary antibodies or replacement of primary antibodies with an isotype-matched IgG_{2a} were used as negative controls.

HRP Histochemistry for Light Microscopy

Retinas incubated with streptavidin-HRP were rinsed and then incubated in 50 ml of Nickel-Tris buffer (pH 7.6) containing 25 mg of diaminobenzidine and 0.1 ml of 3% (v/v) hydrogen peroxide to enhance the generation of the colored HRP reaction product. After 3 minutes of incubation, the retinas were rinsed in PBS to stop the HRP reaction, mounted on gelatin slides, dehydrated through a series of alcohol and xylene solutions, and finally coverslipped with DepeX. The preparations were examined with an Olympus Vanox light microscope.

Intravascular Perfusion with Monastral Blue

To identify activated monocytes and endothelial cells in the retina, some infected animals at day 7 p.i. were kept warm for 20 minutes before tail vein injection with 200 μl of Monastral blue dye (Sigma M3764, containing 3% particulate matter).[16] After 60 minutes at room temperature, the animals were sacrificed by cervical dislocation. The procedures for retinal whole-mount preparation and immunostaining with ICAM-1 and VCAM-1 were as described above.

Quantitative and Densitometric Analysis of ICAM-1 and VCAM-1 Expression

To quantify the expression of the cellular adhesion molecules ICAM-1 and VCAM-1 on retinal blood vessels, whole-mount preparations from control CBA and CBA-PbA mice were examined at days 3, 5, and 7 p.i. (n = 12 in each group). Six of these preparations in each group were photographed using an Olympus Vanox research microscope (20× objective, with 2.5× tube factor) with Kodak Ektachrome 64 color reversal film. The fields selected for quantification with densitometry included the central 0.24 mm^2 surrounding the optic disc. Densitometric analysis of cellular adhesion molecule expression was carried out only for retinal veins, because the narrow lumens of arteries prevented accurate analysis using densitometry. The retinal veins were clearly distinguishable from arteries because of their wider caliber. In addition, the retinal veins were seen to coalesce at the optic nerve head to form the central retinal vein.

The images were scanned with a personal densitometer (Molecular Dynamics Co.) with ImageQuant (Microsoft version 3.2) software. For each vein analyzed, the optical density reading for a region of the parenchyma (without any vessels or artifacts) was measured and subtracted from the optical density measured inside the lumen of the vein, within an area of 0.24 mm^2 surrounding the disc. Optical densities of five to six veins in each retina were measured, and the mean was calculated for each time point. The mean optical density for each observation period was compared with control animals, using the Wilcoxon two-sample rank test. P values <0.05 were considered statistically significant.

Results

Macroscopic Changes in Retinal Vascular Permeability during FMCM

Using intravascular perfusion of HRP, no evidence of blood-retinal barrier breakdown was evident in control CBA mouse retinas (Figure 1A). The HRP reaction product was retained within the vascular lumen, and no HRP was evident in the parenchyma. By day 3 p.i., focal areas of HRP leakage were seen (Figure 1B). By day 5 p.i., an increasingly severe breakdown of the blood-retinal barrier was evident (Figure 1C). Extravascular HRP product was extensively seen in the retinas of CBA-PbA mice on day 7 p.i., at which time animals were dying with obvious cerebral complications. These vascular permeability changes

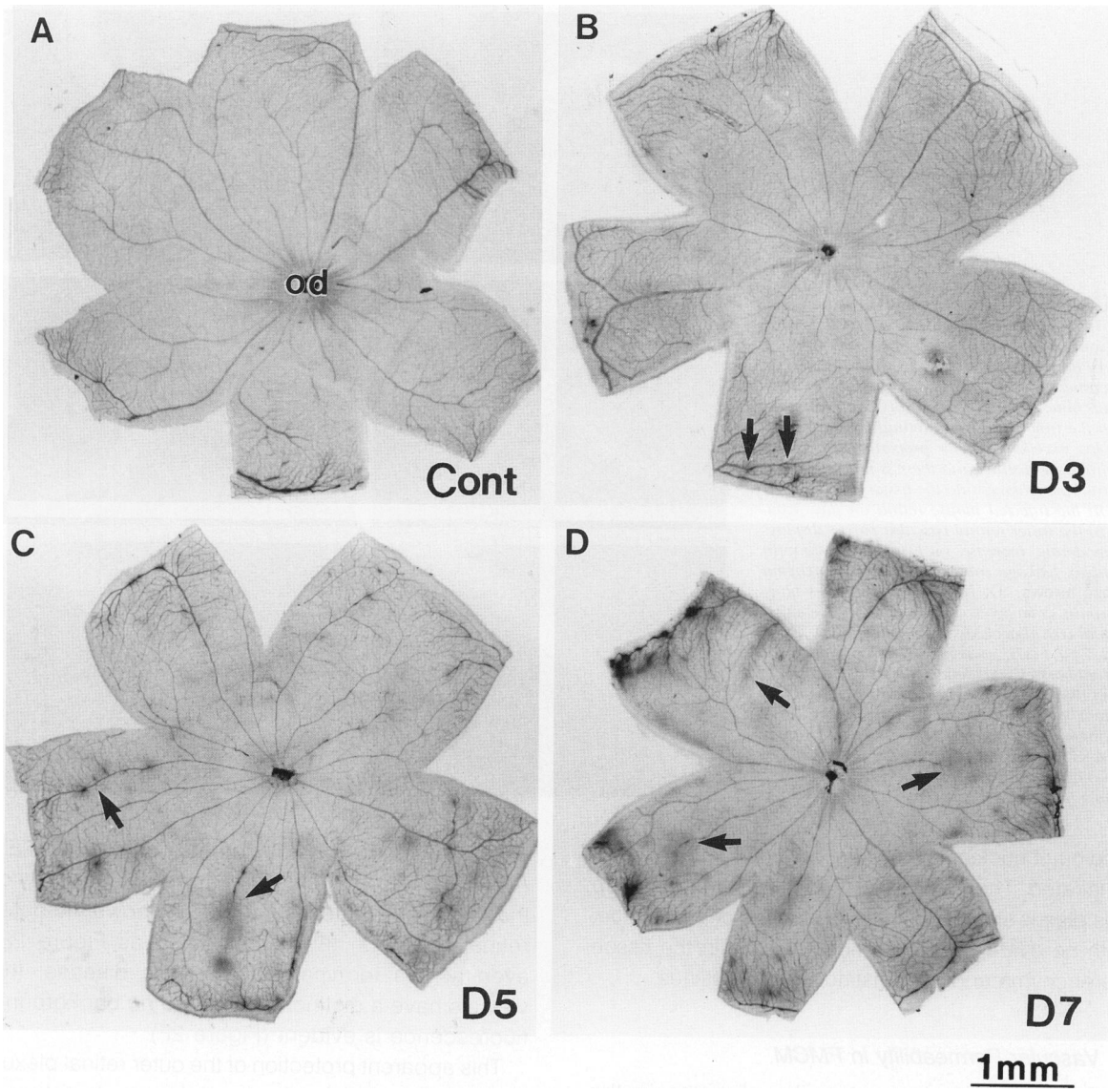

Figure 1. *HRP leakage in flat-mounted retinas of control mice and in infected mice during the progression of FMCM. Animals were not perfused intravascularly before sacrifice.* A: *Control mouse. After intravascular injection with HRP, the brown-black HRP product is visible within the retinal vasculature, but there is no HRP leakage from the vessels.* B: *In CBA-PbA mice on day 3 p.i. (D3), increased HRP leakage in the retina is sometimes seen focally* (arrows). C: *By day 5 p.i. (D5), HRP leakage in the retina is quite extensive* (arrows). D: *By day 7 p.i. (D7), there is a dramatic increase in HRP leakage in mid-peripheral regions* (arrows). *As a consequence of HRP leakage, the clarity of the vessel outline is lost and the intensity of HRP inside the vessel lumen diminished* (C *and* D). *The background staining intensity also increases with increasing disease severity* (B *to* D). *od, optic disc. Scale bar, 1 mm.*

were more often found in the mid-peripheral regions of the retina (Figure 1D).

Light Microscopic Changes in Retinal Vascular Permeability to Evans Blue during FMCM

Vascular Permeability in Uninfected CBA Mice

Vascular permeability to protein was assessed in control animals by intravascular injection of Evans blue to visualize sites of barrier breakdown to the Evans Blue-albumin complex and showed no evidence of leakage in either the inner or outer retinal plexus. The inner retinal plexus, found in the ganglion cell and nerve fiber layers, consists of arteries, arterioles, capillaries, venules, and veins. Figure 2A shows the inner retinal plexus in control uninfected mice, which was characterized by vessels with a very distinct outline due to retention of Evans blue within the vascular lumen. Figure 2B shows the same region of the retina as shown in Figure 2A but now focused at the junction of the outer plexiform layer

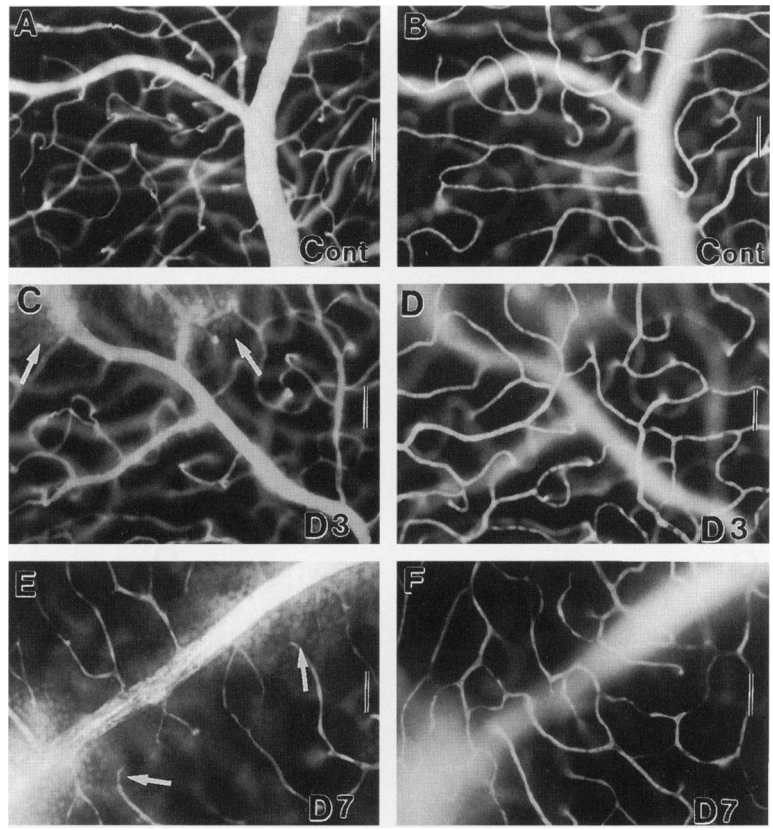

Figure 2. *The integrity of the blood-retinal barrier in the inner and outer retinal vascular plexi in control uninfected CBA mice and infected CBA-PbA mice on days 3, 5, and 7 p.i. was examined by intravascular perfusion with Evans blue.* **A** *and* **B:** *In control (Cont) animals, both the inner and outer retinal vascular plexi display excellent barrier properties. The vessel outlines are distinct and there is no evidence of Evans blue leakage into the tissue parenchyma.* **C:** *In the infected mouse retina on day 3 p.i. (D3), the inner retinal vascular plexus displays a moderate increase in Evans blue-albumin complex leakage into the retinal parenchyma* (white arrows). **D:** *Leakage of the Evans blue-albumin complex is not evident in the outer retinal vascular plexus (same field as* **C**). **E:** *By day 7 p.i. (D7), gross breakdown of the blood-retinal barrier is evident. Leakage of Evans blue from the lumen of inner retinal vessels into the parenchyma is obvious. As a result, the vessel outlines appear blurred* (arrows). **F:** *In contrast, there is no evidence of leakage of Evans blue in the outer retinal vascular plexus at day 7 p.i. (same field as* **E**). *Scale bars, 10 μm.*

and outer nuclear layer where the outer retinal plexus is located. The capillary-sized vessels that make up this plexus showed excellent retention of Evans blue, with no evidence of dye fluorescence in the tissue parenchyma and very distinct vessel outlines.

Vascular Permeability in FMCM

Our earlier work on vascular changes in the retina between days 2 and 3 p.i. has shown a small but reproducibly detectable increase in the level of extravasated Evans blue, despite there being no obvious sites of focal leakage.[16] In the current study, by day 3 p.i., the inner retinal vascular plexus displayed obvious sites of Evans blue leakage (Figure 2C), although the frequency of these sites was limited. However, in contrast to the inner retinal plexus, the outer retinal plexus showed no detectable changes in vascular permeability to the Evans blue-albumin complex (Figure 2D, same area as Figure 2C). This loss of barrier properties in the inner retinal plexus increased from day 3 p.i., peaking at day 7 p.i., the fatal stage of the disease (Figure 2E). By day 7 p.i., Evans blue distribution indicated a dramatic increase in plasma albumin leakage to the extravascular space from the inner retinal vascular plexus, which also had poor plasma perfusion (Figure 2E). Again, we were struck by the apparent normality of the outer retinal plexus. Figure 2F shows the outer retinal plexus in the same region as Figure 2E; even at this terminal stage of the disease, the vessels have a distinct outline and no background fluorescence is evident (Figure 2F).

This apparent protection of the outer retinal plexus from blood-retinal barrier breakdown led us to explore further the mechanism behind this difference in the vascular response between two vascular plexi from the same tissue.

Retinal Histopathological Changes during FMCM

The inner retinal vascular plexus is located within the nerve fiber and ganglion cell layer (Figure 3A), whereas the outer retinal vascular plexus is located at the border of the inner nuclear layer and the outer plexiform layer (empty arrowhead in Figure 3A). In control CBA mice, HRP was not visible within the vessel lumen or in the surrounding tissue (Figure 3A). As indicated by distribution of Evans blue, the inner and outer retinal vascular plexi displayed different responses during the progression of FMCM. No detectable changes were evident from histolog-

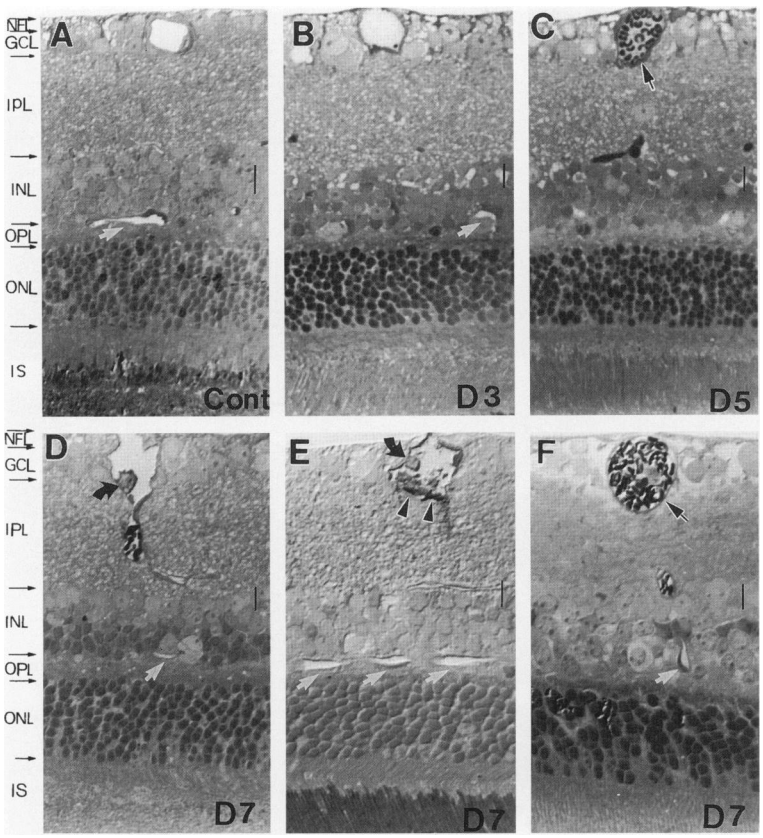

Figure 3. *Transverse sections (0.5 μm, stained with toluidine blue) comparing the inner and outer retinal vascular plexi in control (Cont) and infected mice on days 3, 5, and 7 p.i. (D3, D5, D7). The inner retinal vascular plexus is located in the nerve fiber layer (NFL) and the ganglion cell layer (GCL). The outer retinal vascular plexus is located at the junction of the inner nuclear layer (INL) and the outer plexiform layer (OPL). IPL, inner plexiform layer; ONL, outer nuclear layer; IS, inner segments of the photoreceptors.* **A:** *The lumens of both the inner and outer retinal vascular plexi are empty after intravascular perfusion with PBS. In control animals, HRP product is not evident inside the vascular lumen or in the parenchyma.* **B:** *By day 3 p.i., a low level of extracellular edema is evident in the inner retinal layers.* **C:** *By day 5 p.i., some inner retinal vessels are congested with red blood cells* (small arrow). **D** *and* **F:** *By day 7 p.i., adherent monocytes* (curved arrows) *are seen in the inner retinal vascular plexus, and some vessels are congested* (small arrow). *Marked edema is seen in the NFL and GCL at day 7 p.i. HRP leakage into the parenchyma is also visible in the inner retinal plexus* (arrowheads). *In contrast, throughout the malaria infection, the outer retinal vascular plexus* (white arrows) *appears similar to controls* (**B** *to* **F**). *Scale bars, 10 μm.*

ical sections at day 3 p.i. (Figure 3B). However, by day 5 p.i., mild edema was evident in the ganglion cell, nerve fiber, and inner plexiform layers, and vessels congested with red blood cells were evident in the inner retinal plexus (arrow in Figure 3C). At day 7 p.i., HRP reaction product was seen outside the vessel lumen in some areas (arrowheads in Figure 3E). Adherent monocytes were frequently observed coated with HRP (curved arrows in Figure 3, D and E). Congested vessels with various blood components were also observed in the inner retinal plexus (Figure 3F). The extent of extracellular edema in the ganglion cell and nerve fiber layers increased with the progression of the disease. However, these pathological features seen in the inner retinal vascular plexus were not detectable in the outer retinal vascular plexus in infected animals even at the terminal stage of the disease (Figure 3, D–F).

Cellular Responses during FMCM

Uninfected CBA Mice

In control mice injected with HRP, both the inner and outer retinal vascular plexi maintained their structural integrity to HRP (Figure 4, A–D), characterized by tight junctions between adjacent vascular endothelial cells. The inner retinal vessels were surrounded by a continuous basement membrane and ensheathed by the processes of Müller cells and astrocytes (Figure 4B). In contrast, only Müller cell processes ensheathed the outer retinal vessels (Figure 4, C and D). All retinal vessels were empty after intravascular perfusion with Hartmann's solution, and HRP granules were not evident within vascular lumens or adherent to the luminal endothelial surface or in the extravascular spaces (Figure 4, A–D). In contrast to FMCM, there was no evidence of cellular responses such as monocyte adhesion, increased HRP adhesiveness, or endothelial cell damage, as reported below, in control CBA mice.

Cellular Responses in FMCM

There was a remarkable difference in the cellular responses observed between the inner and outer retinal vascular plexi on day 7 p.i. (CBA-PbA). Even after intravascular perfusion with buffer, monocytes were frequently observed adherent to the endothelium of the inner retinal vascular plexus (Figure 5A). Furthermore, the luminal surfaces of the vascular endothelium (Figure 5, B and C) and adherent mono-

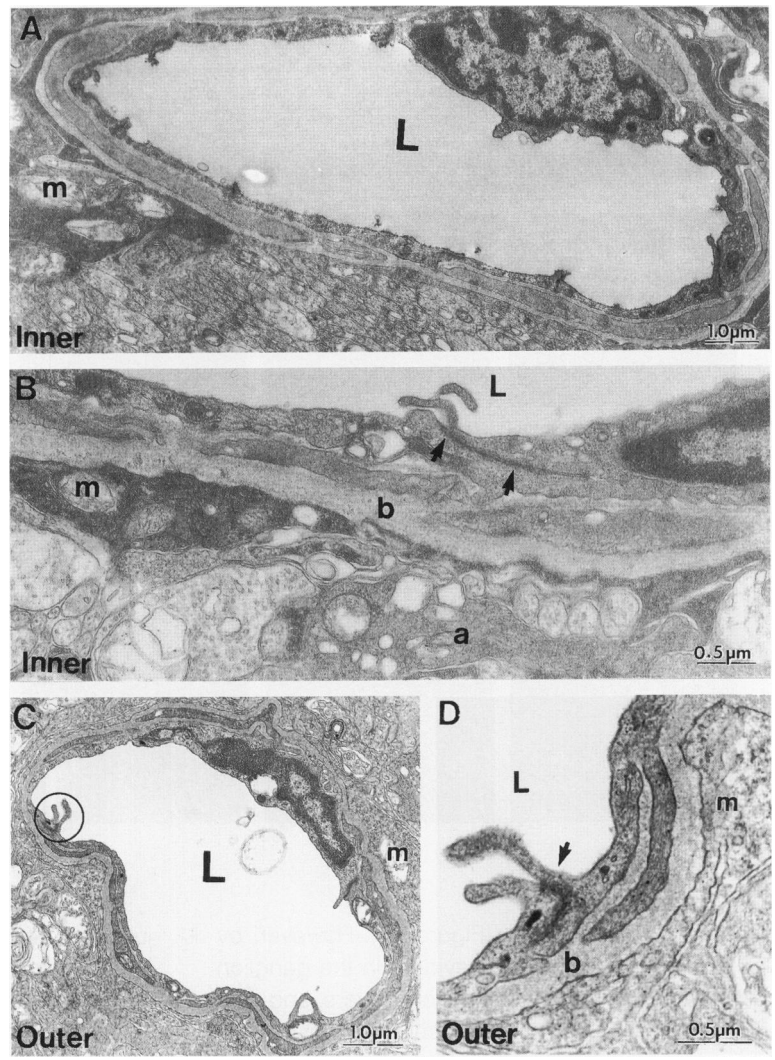

Figure 4. *Ultrastructure of the inner and outer retinal vascular plexi in the control CBA mice after intravascular perfusion with HRP. All of the vessels have empty lumens (L), with no evidence of leakage or HRP adherent to the endothelial surfaces.* A: *An inner retinal vessel is partially wrapped by retinal Müller cell processes (m).* B: *Higher magnification view of an inner retinal vessel, showing a tight junction between adjacent endothelial cells* (arrows), *surrounded by a continuous basement membrane (b). The glia limitans of this vessel are formed by both retinal Müller cell (m) and astrocyte processes (a).* C: *A continuous basement membrane is also evident around the outer retinal vessels, which are ensheathed by Müller cell processes alone (m). The area enclosed by the circle is shown at higher magnification in* D. D: *Tight junction* (arrow) *is evident between adjacent vascular endothelial cells in the outer retinal plexus.*

cytes (Figure 5D) were extensively coated by HRP granules. Adherent monocytes sometimes contained HRP-positive lysosomes (not shown). The surfaces of adherent monocytes displayed ruffled plasma membranes, an observation frequently associated with monocyte activation. Although massive extrusion of HRP into the space between the vascular endothelial cells and the basement membrane was not evident, other observations suggested changes in the status of the blood-retinal barrier. These included HRP granules in subendothelial areas (seen infrequently), HRP-containing vesicles within the cytoplasm of endothelial cells, and endothelial vacuolation (Figure 5, B and C). There was a loss of the junctional complexes normally found between adjacent endothelial cells in the CNS, resulting in HRP granules being found trapped within the junctional complexes between adjacent vascular endothelial cells (Figure 6A). This usually occurred in association with sites of monocyte adhesion. Infrequently, platelets were observed adhering to the vascular endothelium (Figure 6A). Extravasated monocytes were sometimes seen in the parenchyma (Figure 6A) adjacent to inner retinal vessels. Perhaps as a consequence of the vascular permeability changes, edema (Figures 5A and 6A) and hemorrhages (Figure 6B) were also noted at this time in the inner retina of infected animals. In contrast to the extensive vascular responses seen in the inner retinal vascular plexus, the outer retinal vascular plexus exhibited a normal appearance during the course of the disease (eg, Figures 6C and 7, A and B).

Expression of Cellular Adhesion Molecules in Retinal Vessels during FMCM

To further examine the increased adhesiveness for HRP and monocytes of the endothelial luminal sur-

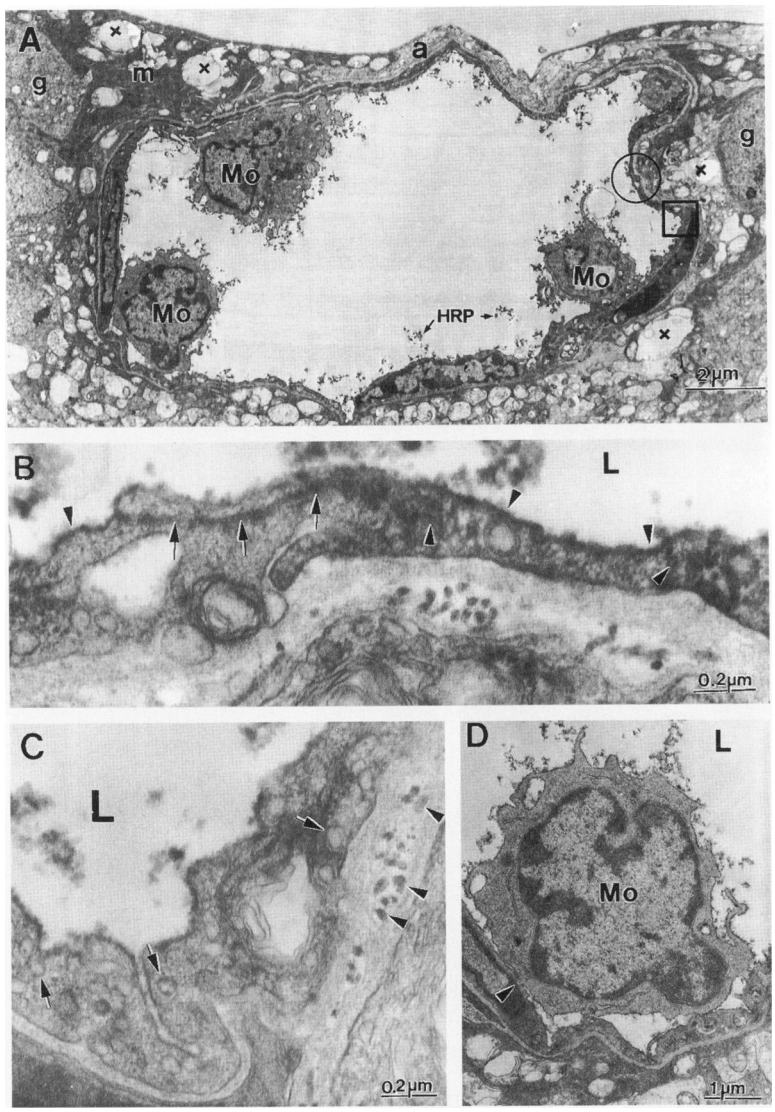

Figure 5. *Electron micrographs showing the inner retinal vascular plexus from a malaria-infected mouse on day 7 p.i.* A: *Monocytes (Mo) are adherent to the vascular endothelium. Some HRP granules* (small arrows) *are visible on the surfaces of monocytes and endothelial cells. Both astrocytes (pale cytoplasm; a) and Müller cells (dark cytoplasm; m) ensheath the inner retinal vessels. The somas of two adjacent ganglion cells (g) are also visible. Extracellular edema (x) is evident throughout the ganglion cell layer.* B: *A higher magnification view of the area encircled in* A *showing a junction between adjacent endothelial cells filled with HRP* (arrows). *The increased adhesiveness of the vascular endothelial cell surface is evident by the coating of the cell surface with HRP whereas abundant HRP is evident in the endothelial cytoplasm* (arrowheads). C: *A higher magnification view of the area within the square from* A. *A marked increase in the number of vesicles* (arrows) *is seen within the endothelial cytoplasm. Leaked HRP granules* (arrowheads) *are evident within the basement membrane surrounding the inner retinal vessel.* D: *High magnification view showing a monocyte from* A *firmly adherent to the vascular endothelial cell. The cytoplasmic membrane of the monocyte (Mo) and vascular endothelial cell appear in close apposition* (arrowhead).

face during FMCM, animals were given an intravenous injection of Monastral blue 1 hour before sacrifice, followed by immunohistochemistry for adhesion molecules known to be expressed on the vascular endothelium, ICAM-1 (antibody YN1/1) and VCAM-1 (antibody MVCAM.A429).

ICAM-1 Expression

In control uninfected CBA mice, the inner retinal vessels showed negligible expression of ICAM-1 in arteries, veins, capillaries, and post-capillary venules (Figures 8A and 9A; Table 1). Between days 3 and 7 p.i., we found that the expression of ICAM-1 increased progressively on veins and venules of the inner retinal plexus (Figures 8, B–D, and 9, B and G), with a lesser increase on arteries and arterioles but none on capillaries (Table 1). However, the outer retinal vascular plexus did not display up-regulation of ICAM-1 expression or any evidence of monocyte adhesion after intravascular injection with Monastral blue in infected animals during the course of the disease (Figure 9H).

By day 7 p.i., the inner retinal veins exhibited a marked increase in ICAM-1 expression, apparently on the endothelial luminal surface, and numerous adherent ICAM-1$^+$ monocytes were observed (Figure 9, C–E). This compared with empty vessel lumens and low basal levels of ICAM-1 expression seen in similar vessels in control animals (Figure 9A). In some vascular segments, there were numerous ICAM-1$^+$ monocytes aggregated within the vessel lumens, some of which appeared to be attached to the endothelium (Figure 9C). Perhaps as a consequence of the monocytes adhering to the vascular endothelium, the blood

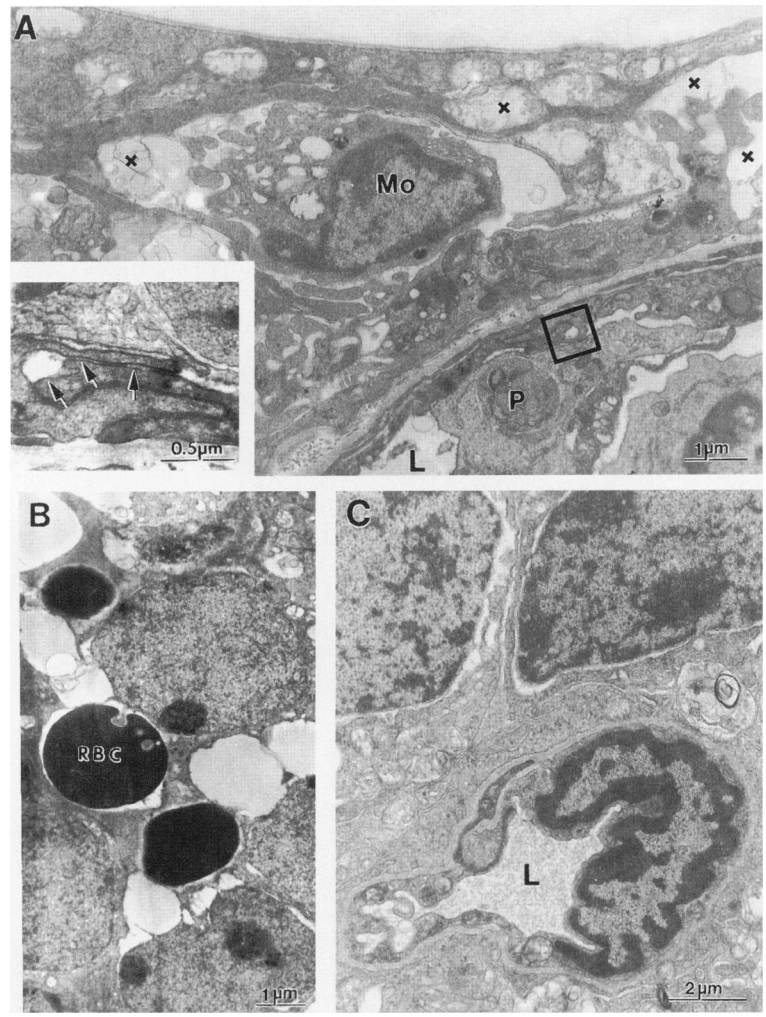

Figure 6. *Electron micrographs of the retina in CBA-PbA mice on day 7 p.i.* A: *Occasionally, platelets (p) are observed adherent to the endothelial surface of the inner retinal vessels. In the perivascular space, a mononuclear cell (Mo) with HRP-positive cytoplasmic granules is visible, and extracellular edema is also evident (x).* Inset: *Higher magnification view of the area within the square shown in* A. *The interendothelial junction next to the adherent platelet shows marked changes including an obvious gap* (arrows) *between the cytoplasmic membranes of adjacent vascular endothelial cells.* B: *Extravasated red blood cells (RBC) are found in the parenchyma, suggestive of a small hemorrhage.* C: *In marked contrast, the outer retinal vessels from a day 7 p.i. animal show no detectable changes. L, lumen.*

perfusion in some vessel segments was severely affected. Many of the ICAM-1$^+$ monocytes had ruffled surfaces and contained numerous dark cytoplasmic granules, presumably HRP granules or phagocytosed malaria pigment (Figure 9D). Infrequently, we observed what appeared to be the extravasation of monocytes into the surrounding parenchyma (Figure 9, E and F).

VCAM-1 Expression

In control CBA mice, VCAM-1 was not expressed on venules and veins (Figures 8E and 10A), although there was some expression on arteries and arterioles (Figures 8E and 10, A and B; Table 1). Between days 3 and 7 p.i. there was a progressive increase in the expression of VCAM-1 on small arteries, arterioles, veins, and venules, peaking at the fatal stage of the disease (Figures 8, F–H, and 10, C–G; Table 1). However, adherent monocytes were VCAM-1 negative. These adherent monocytes were further identified by Monastral blue coating of the monocyte surface (Figure 10F). Compared with these marked changes seen in the inner retinal vascular plexus during the progression of FMCM, there was a complete absence of VCAM-1 expression and monocyte adhesion in the outer retinal vascular plexus, even at the terminal stage of the disease (day 7 p.i.; Figure 10H).

Quantitative and Semiquantitative Analysis of ICAM-1 and VCAM-1 Expression during FMCM

The degree of increased expression of ICAM-1 and VCAM-1 varied in specific vascular segments (Table 1). Furthermore, using densitometry, the level of VCAM-1 expression revealed by immunohistochemistry on the inner retinal veins was found to be significantly increased at day 3 p.i. in CBA-PbA mice, compared with control animals ($P = 0.01$; Figure 11). This is 2 days earlier than that indicated from our subjective grading assessment of VCAM-1 expression, suggest-

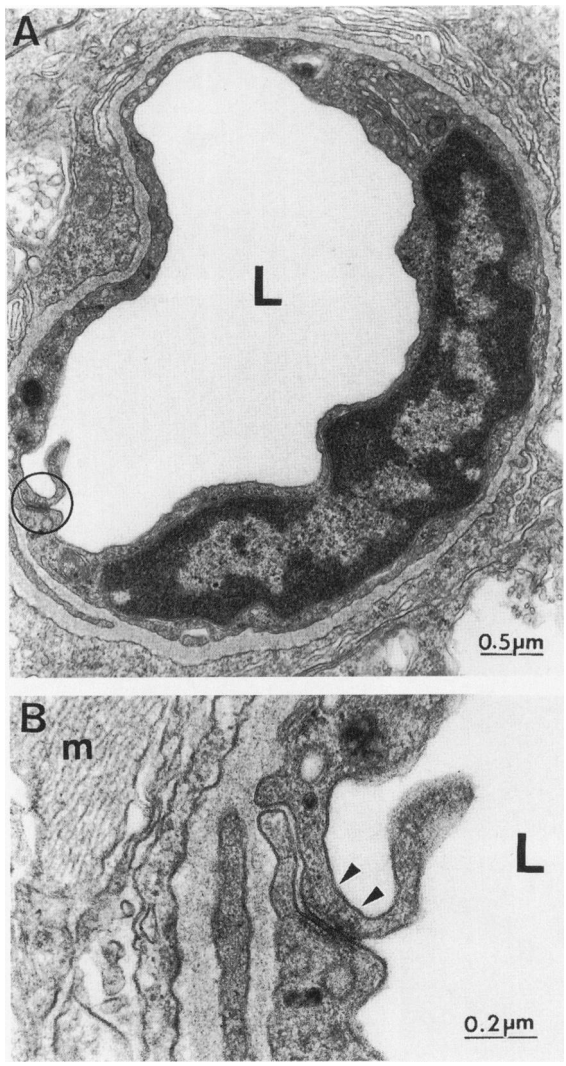

Figure 7. A: *A high magnification view of an outer retinal vessel at day 7 p.i. showing no coating of the vessel lumen (L) with HRP, normal vascular endothelial morphology, and absence of adherent monocytes.* B: *A higher magnification view of the area encircled in* A *showing a tight junction* (arrowheads) *between adjacent vascular endothelial cells. This vessel is surrounded by a continuous basement membrane and ensheathed by Müller cell processes (m).*

ing that densitometry is more sensitive at detecting slight increases of VCAM-1 expression. The density of ICAM-1 staining in these sites at day 3 p.i. displayed no significant change when compared with the controls ($P > 0.05$; Figure 11). However, at days 5 and 7 p.i., the density of both ICAM-1 and VCAM-1 staining on the inner retinal veins was significantly increased compared with controls ($P = 0.005$).

Discussion

We previously have demonstrated the advantages of the retinal whole-mount system for studying the interaction of immune system components with the CNS microvasculature in FMCM.[16,17,34] Using this technique, it is possible to co-visualize changes in parameters such as microvascular permeability with the distribution and properties of blood leukocytes,[16,17] astrocytes,[34] and microglia (I. M. Medana, N. H. Hunt, and T. Chan-Ling, manuscript submitted). A precise correlation of such changes with the pattern of response in the brain has been demonstrated,[16,17] but the retinal observations also have revealed certain significant changes in the microcirculation earlier in the course of pathogenesis than had formerly been possible and have allowed the study of critical cell-cell interactions in FMCM.

Confirming our earlier observations,[16,17] an increase in the permeability to protein of the blood-retinal barrier was seen by days 2 to 3 p.i. during the pathogenesis of FMCM. However, we now have shown that this change occurred only in the inner vascular plexus. At approximately the same time, in specific regions of the retinal microcirculation there commenced a progressive up-regulation of the expression of the adhesion molecule VCAM-1 (Figure 11). Endothelial ICAM-1 expression was up-regulated by day 5 p.i., coincident with the appearance of ICAM-1$^+$ monocytes adhering in the same areas of the retinal microvasculature. The start of the monocyte adherence coincided with the first signs of neurological symptoms in the animals. The increased vascular permeability, the expression of adhesion molecules, and monocyte adherence to the endothelium were all very prominent features at the time the animals went into coma and died. The temporal sequence of these vascular changes in the inner retinal vascular plexus, together with their complete absence in the outer retinal vascular plexus, suggests that they may be mechanistically interrelated.

A number of factors could explain the differential response between the inner and outer retinal plexi. First, both astrocytes and Müller cells contribute to the glial ensheathment of the vessels in the inner plexus, whereas only Müller cells ensheath the outer retinal vessels.[35] We previously have shown that astrocyte changes occur early in FMCM and may be related to the breakdown of the blood-retina barrier[34] and that retinal astrocytes are very sensitive to hypoxic insult in the feline model of retinopathy of prematurity, whereas Müller cells are not affected.[31] Thus, a difference in the vascular response between the inner and outer vascular plexi could be due to a difference in the susceptibility to damage of the glial cells that form their glia limitans.

A second difference between the two vascular plexi is the absence of larger vessels in the outer bed, which consists predominantly of capillary-sized

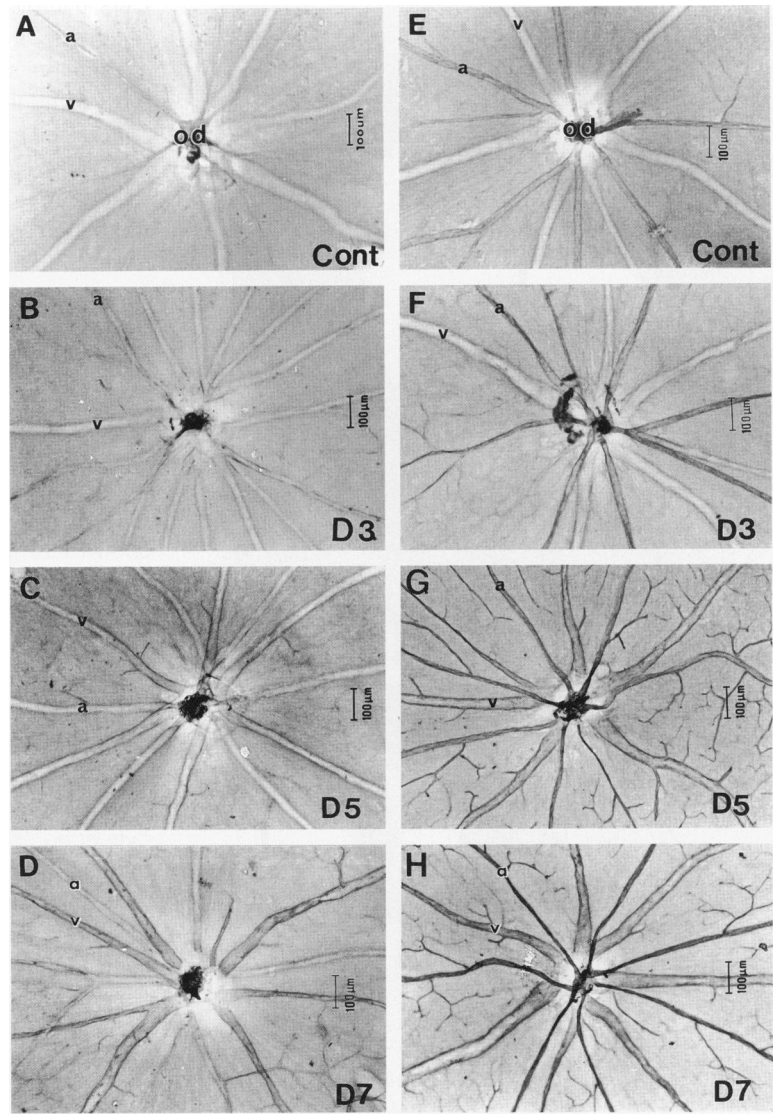

Figure 8. *Immunoreactivity of adhesion molecules, ICAM-1 and VCAM-1, in retinal whole mounts during the progression of FMCM. The regions shown include an approximate 0.9 × 1.2 mm² area surrounding the optic disc (od).* **A:** *In control animals, a very low level of ICAM-1 immunoreactivity is seen in the major arteries (a) and veins (v) around the optic disc.* **B** *to* **D:** *The intensity of ICAM-1 immunoreactivity in the venules and veins progressively increases between days 3 and 7 p.i. (D3, D5, D7).* **E:** *In control animals, VCAM-1 immunoreactivity is higher in retinal arteries compared with retinal veins (v). This contrasts with constitutive expression of ICAM, which is low for both arteries and veins* (**A**). **F** *to* **H:** *Between days 3 and 7 p.i. the immunoreactivity of VCAM-1 in venules and veins is progressively increased.*

vessels. Few changes were observed in the capillaries of the inner retinal plexus, so the different natures of the two vascular beds may underlie the dissimilarity in their responses during FMCM.

Increased Retinal Vascular Permeability in FMCM

Extravasation of the Evans blue-albumin complex commenced at or before day 3 p.i. and was almost completely restricted to the inner retinal vascular plexus. The outer retinal vascular plexus, mainly composed of capillary-sized vessels, did not display increased vascular permeability to Evans blue-protein at any time during the course of FMCM. Intravascular administration of HRP was used for the first time in this model as another index of increased vascular permeability to macromolecules. HRP leakage from the microcirculation was visible macroscopically. Leakage of this macromolecule specifically from the inner retinal vascular plexus was seen microscopically and, to a lesser extent, by electron microscopy. The occurrence of edema, evident histologically in retinal sections and by electron microscopy, was consistent with these findings.

The blood-retinal barrier forms a selective cellular interface between the blood and the retinal parenchyma and is functionally identical with the blood-brain barrier.[36] In contrast to the peripheral circulation, the endothelial cells of the retinal microcirculation form and maintain tight, impermeable junctions between them and express a very low rate of pinocytotic activity to restrict the movement of polar solutes and to control the

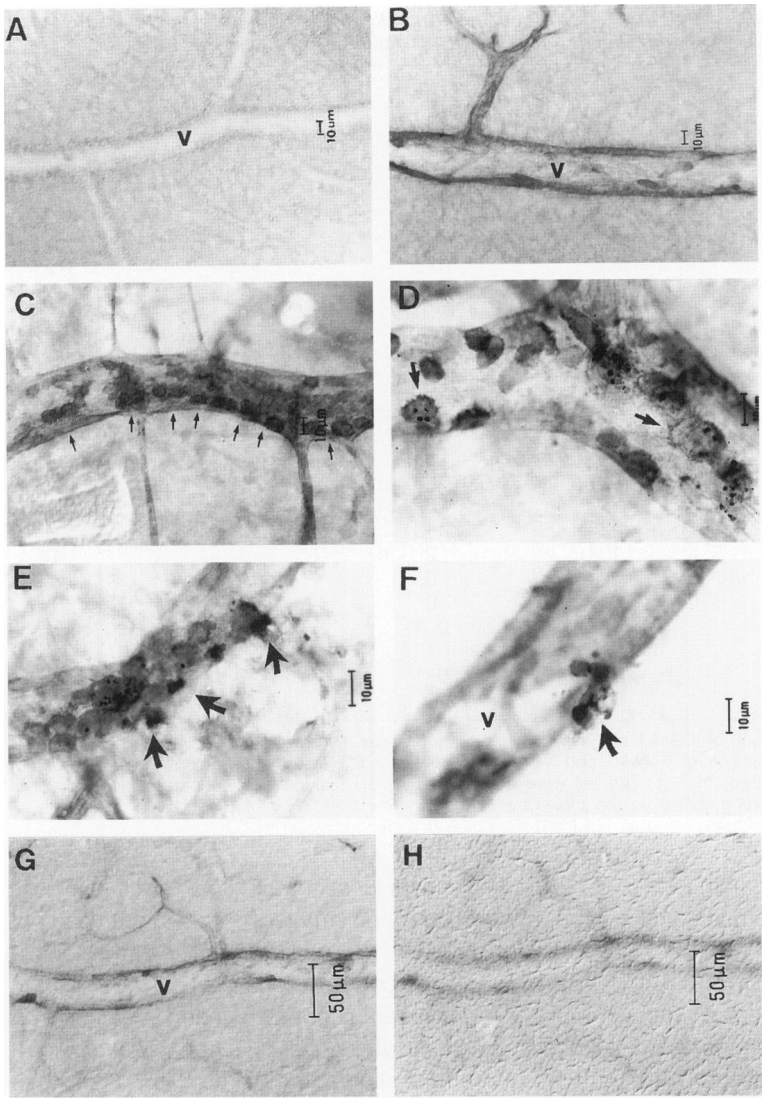

Figure 9. *High magnification views showing changes of ICAM-1 immunoreactivity in retinal whole mounts during FMCM.* A: *Very low level of ICAM-1 immunoreactivity in a retinal vein (v) in control CBA mice.* B: *By the fatal stage of the disease (day 7 p.i.), a marked increase in the immunoreactivity of ICAM-1 is evident in retinal veins (v).* C: *A retinal vein (v) showing a number of ICAM-1$^+$ monocytes marginated along the vessel wall* (arrows). D: *Some adherent monocytes have a ruffled surface and contain dark granules (presumably HRP granules or malaria pigment).* E *and* F: *A number of monocytes are aggregated within the lumen of a vein. On rare occasions, shown in* E *and* F, *monocytes are seen in the process of traversing the vessel wall* (arrows). G *and* H: *Same region of the retina after immunohistochemistry for ICAM-1 at day 7 p.i. The inner retinal vein is ICAM-1 positive* (G) *whereas the outer retinal vascular plexus at the inner nuclear layer, focused by Nomarski optics, is ICAM-1 negative* (H).

extravasation of blood components under normal circumstances.[36] An intact basement membrane and glia limitans, contributed by Müller cells and astrocyte processes, are also necessary to maintain the integrity of the blood-retinal barrier.[35] At the terminal stage of FMCM, electron microscopy revealed, in the inner retinal vascular plexus only, disruption of tight junctions and an increased incidence of pinocytotic vesicles and vacuolation. We previously have shown, by immunohistochemistry, astrocyte redistribution occurring early in the course of FMCM and some loss of these glial cells at the terminal stage.[34] It was concluded that the early redistribution was a consequence of the increase in microvascular permeability to protein, whereas the loss of astrocytes was a consequence of activation of an immunopathological process.[34]

Two different patterns of increased vascular permeability to macromolecules in the CNS during the course of FMCM have been reported by us.[13,14,16,17] Initially, there is a mild change, seen as early as day 2 p.i., which is overwhelmed by a massive increase starting at approximately day 5 p.i. The process that initiates the early increase is unclear, but it is possible that a parasite product directly interacts with the endothelium. Factors released from, or associated with, parasitized erythrocytes are capable of stimulating nitric oxide release by endothelial cells.[37,38] The increased movement of plasma proteins into the CNS early on during the pathogenesis of FMCM seems likely to be the factor that induces concurrent changes in the distribution and morphology of astrocytes[34] and microglia (I. M. Medana, N. H. Hunt, and T. Chan-Ling, manuscript submitted).

It has been suggested that extravasation of plasma proteins in the CNS in various pathological conditions may occur via a number of different

Table 1. *Subjective Grading of Expression of ICAM-1 and VCAM-1 on the Inner Retinal Vasculature in Whole-Mount Preparations in Uninfected, Control Mice and Others Infected with* Plasmodium berghei *ANKA*

Site	Range (R) and Mode (M)	Control	CBA-PbA Day 3	CBA-PbA Day 5	CBA-PbA Day 7
ICAM-1					
Arteries	(R)	0–1*	0–1	1–2‡	1–3§
	(M)	0	1	1	1
Arterioles	R	0*	0–1†	1–2§	1–2§
	M	0	1	1	2
Capillaries	R	0*	0	0	0
	M	0	0	0	0
Venules	R	0*	0–1	1–2‡	2–3§
	M	0	0	2	3
Veins	R	0*	0–1	1–2§	3–4§
	M	0	1	2	3
VCAM-1					
Arteries	R	1–2	1–3	2–4§	3–4§
	M	2	3	4	4
Arterioles	R	1–2	1–3	2–4§	3–4§
	M	1	2	3	4
Capillaries	R	0	0	0	0
	M	0	0	0	0
Venules	R	0	0–1	1–3§	3–4§
	M	0	1	3	4
Veins	R	0	0–1	2–4§	3–4§
	M	0	1	3	4

The changes in the vascular endothelial expression of ICAM-1 and VCAM-1 in each individual retina were graded as follows: 0, lowest level of expression seen; 1 to 4, increased expression of ICAM-1 and VCAM-1, from slight (1) to the most intense (4). Number of observations per group = 12, except where indicated; *n = 11. Values were compared by the Kruskal-Wallis nonparametric analysis of variance test. Significant differences from corresponding control values shown by $^{\dagger}P < 0.05$; $^{\ddagger}P < 0.01$; $^{\S}P < 0.001$.

routes, including diffusion through altered tight junctions, increased pinocytosis, or the formation of transendothelial channels (reviewed in Ref. 39). From our ultrastructural observations on day 7 p.i., it seems likely that the increased incidence of junctional gaps and endothelial vacuolation in the inner retinal vascular plexus serve as major routes through which extravasation of blood albumin and intravascular tracers such as HRP occur during the late stage of FMCM. Frankly damaged endothelial cells also have been observed,[13,17] sometimes situated adjacent to monocytes. These areas of focal damage may be the source of the petechial hemorrhages that are characteristic of FMCM and human CM.

It is likely that the severe, widespread breakdown of the blood-brain barrier that occurs late in the course of FMCM is a consequence of the activation of cellular components of the immune system. The pathogenesis of FMCM is known to depend on $CD4^+$ T lymphocytes and a number of cytokines, including tumor necrosis factor (TNF).[40,41] Administration to normal animals of interferon-γ and TNF-α can cause disruption of the blood-brain barrier and the blood-retinal barrier,[39,42] and both of these cytokines are thought to play a role in FMCM as antibodies against them protect against the cerebral complications.[40] Intraocular injection of TNF caused vacuolation and disruption of tight junctions in retinal endothelial cells in rabbits.[42] High plasma levels of TNF are seen not only in FMCM[22,43,44] but also in malaria infections in which cerebral complications are not observed.[44] Thus, it has been suggested that TNF produced locally by monocytes adhering to the cerebral microvascular endothelium may be more important than systemic TNF in FMCM.[44] Recent work from our laboratory has found that TNF is produced by microglia as well as monocytes during FMCM (I. M. Medana, N. M. Hunt, and G. Chaudhri, unpublished). A possible role for phagocyte-derived reactive oxygen species in causing damage to the endothelium in FMCM also has been suggested.[18]

Monocytes and Endothelial Expression of Adhesion Molecules

Monocytes start to adhere to the CNS microvascular endothelium at approximately day 5 p.i. with *P. berghei* ANKA.[14,16] We now have shown that such adherence occurs in the inner retinal vascular plexus but not in the outer retinal vascular plexus, coinciding both temporally and spatially with the pattern of severely increased vascular permeability to plasma proteins and the increased expression of the adhe-

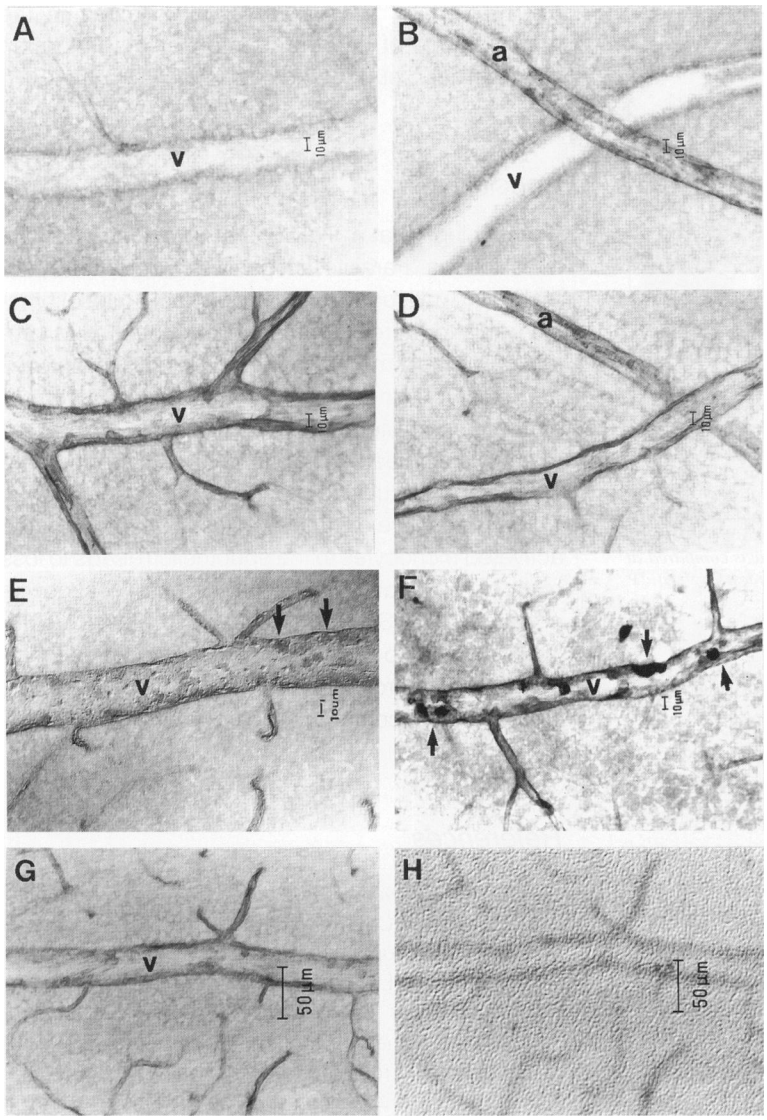

Figure 10. *High magnification views showing changes of VCAM-1 immunoreactivity in retinal whole mounts during FMCM.* A: *Very low level of VCAM-1 immunoreactivity in a retinal vein (v) in control CBA mice.* B: *In contrast to ICAM-1 expression, VCAM-1 is expressed at a higher level in arteries even in control animals. By the fatal stage of the disease (day 7 p.i.), a marked increase in the immunoreactivity of ICAM-1 is evident in retinal veins (v).* C *and* D: *The increased immunoreactivity of VCAM-1 at the fatal stage of FMCM is marked in veins, whereas for arteries the level of immunoreactivity appears similar to control animals.* E: *By day 7 p.i., the adherent monocytes visible with Nomarski optics are VCAM-1 negative* (arrows). F: *In a retinal whole-mount where the monocytes are identified by intravascular injection with Monastral blue before sacrifice. Monastral-blue-positive monocytes are evident within the lumen, adherent to VCAM-1-positive vascular endothelium.* G *and* H: *Same region of the retina after immunohistochemistry for VCAM-1 at day 7 p.i. The inner retinal vein is VCAM-1 positive* (G) *whereas the outer retinal vascular plexus at the inner nuclear layer, focused by Nomarski optics, is VCAM-1 negative* (H).

sion molecules. Electron microscopy revealed that the adherent monocytes had several characteristics associated with an activated state, for example, ruffled membranes, coating with HRP, and the presence of HRP^+ lysosomes. The close juxtaposition of activated monocytes capable of secreting TNF and reactive oxygen species and the endothelium could contribute to impairment of CNS barrier function.

Inasmuch as in other situations the adherence of monocytes to the endothelium is a consequence of the expression of appropriate adhesion molecules, we examined the distribution of ICAM-1 and VCAM-1 on the retinal microvascular endothelium during the course of FMCM. VCAM-1 showed a low level of constitutive expression on arteries in uninfected mice, but ICAM-1 did not. There was a substantial up-regulation of the expression of both molecules in the inner retinal vascular plexus, starting as early as day 3 p.i. and increasing progressively during the course of FMCM. Neither molecule was expressed in the outer retinal vascular plexus at any stage.

Human CNS endothelial cells constitutively express ICAM-1 in culture, and this is up-regulated by TNF and interferon-γ.[45] *P. falciparum*-infected erythrocytes bind to ICAM-1 and VCAM-1 *in vitro*, and the latter molecule is up-regulated on CNS endothelial cells in some CM victims.[25] Thus, an immunopathological process in human CM leads to adherence of parasitized erythrocytes to the microvascular endothelium in the CNS, whereas in FMCM a broadly similar process leads to adherence of monocytes. In both cases, vascular obstruction may result.[16,46] Obstruction of small vessels by mononuclear cells also has been reported in human CM.[11] The significance

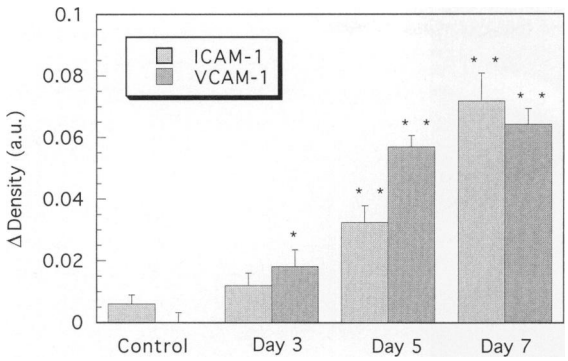

Figure 11. *The intensity of ICAM-1 and VCAM-1 staining in retinal veins is quantified by densitometry during the progression of FMCM. For each measurement, the optical density in a parenchymal region without vessels was subtracted from the optical density within the vein. The intensity of ICAM-1 and VCAM-1 immunoreactivity was determined in five to six veins per retina. The value of each column represents the mean of six animals per condition, and vertical bars indicate the SEM. The difference in immunoreactivity of VCAM-1 and ICAM-1 between control and malaria-infected mice was compared at each time point using the Wilcoxon two-sample rank test* ($n = 6$). *P = 0.01; **P = 0.005.

of vascular occlusion in the development of neuronal dysfunction in human CM is hotly debated.[6,9]

Although others have shown up-regulation of ICAM-1 on the endothelium in the brain during the advanced stages of FMCM,[47] the current study is the first to demonstrate that the increased expression of ICAM-1 and VCAM-1 starts early in the course of the disease. Administration of an antibody against LFA-1 (the ligand of ICAM-1) is protective against FMCM, even if given when neurological symptoms are already established.[47,48] Curiously, administration of anti-ICAM-1 rapidly caused death in these mice, although not in uninfected controls.[47] TNF and interferon-γ can induce ICAM-1 expression on endothelial cells.[45] However, increased circulating levels of TNF[22,41] and expression of TNF mRNA in monocytes and microglia (I. M. Medana, N. M. Hunt, and G. Chaudhri, unpublished) are only detectable from approximately day 5 p.i. onward in this model, 2 days later than the start of increased endothelial expression of ICAM-1. Although it is possible that undetectably low concentrations of cytokines do induce the early expression of these adhesion molecules, it may be that parasite products directly initiate this process, with reinforcement later in the disease process through TNF or other cytokines released by monocytes in close proximity to the endothelium. Up-regulation of these adhesion molecules would enhance adhesion of monocytes, and perhaps platelets,[49] to the CNS endothelium. Parasite products can directly stimulate expression of adhesion molecules and nitric oxide production by endothelial cells[37] and TNF and nitric oxide release by macrophages.[50,51] A role for nitric oxide in the manifestation of cerebral complications in human CM has been suggested.[9]

Conclusions

We conclude that a likely course of events in FMCM is as follows. Parasite antigens stimulate the endothelium to up-regulate adhesion molecule expression and to increase vascular permeability to proteins. The movement of protein into the CNS initiates the redistribution of astrocytes and microglia. Concurrently, parasite antigens activate the cellular immune system, leading eventually to activation of microglia and circulating monocytes for production of TNF and reactive oxygen species. Adherence of the activated monocytes to the endothelium leads to loss of endothelial viability and multiple focal breakdowns of the blood-CNS barrier. Access of proteins, including cytokines, to the CNS parenchyma leads to impairment of neuronal function, manifested as behavioral changes, coma, and death.

References

1. Oo MM, Aikawa M, Than T, Aye TM, Myint PT, Igarashi I, Schoene WC: Human cerebral malaria: a pathology study. J Neuropathol Exp Neurol 1987, 46:223–231
2. Pongponratn E, Riganti M, Punpoowong B, Aikawa M: Microvascular sequestration of parasitized erythrocytes in human falciparum malaria: a pathological study. Am J Trop Med Hyg 1991, 44:168–175
3. Osuntokun BO: Malaria and the nervous system. Afr J Med Med Sci 1983, 12:165–172
4. Toro G, Roman G: Cerebral malaria: disseminated vasculomyelinopathy. Arch Neurol 1978, 35:271–275
5. Warrell DA, Veal N, Chanthavanich P, Karbwang J, White NJ, Looareesuwan S, Phillips RE, Pongpaew P: Cerebral anaerobic glycolysis and reduced cerebral oxygen transport in human cerebral malaria. Lancet 1988, 2:534–537
6. Berendt AR, Turner GDH, Newbold CI: Cerebral malaria: the sequestration hypothesis. Parasitol Today 1994, 10:412–414
7. Grau GE, Taylor TE, Molyneux ME, Wirima JJ, Vassalli P, Hommel M, Lambert PH: Tumor necrosis factor and disease severity in children with falciparum malaria. N Engl J Med 1989, 320:1586–1591
8. Butcher GA, Garland T, Ajdukeiwicz A, Clark IA: Serum tumor necrosis factor associated with malaria in patients in the Solomon Islands. Trans R Soc Trop Med Hyg 1990, 84:658–661
9. Clark IA, Rockett KA: The cytokine theory of human cerebral malaria. Parasitol Today 1994, 10:410–412

10. Grau GE, De Kossodo S: Cerebral malaria: mediators, mechanical obstruction or more? Parasitol Today 1994, 10:408–410
11. Patnaik JK, Das BS, Mishra SK, Mohanty S, Satpathy SK, Mohanty D: Vascular clogging, mononuclear cell margination, and enhanced pathogenesis of human cerebral malaria. Am J Trop Med Hyg 1994, 51:642–647
12. Rest JR: Cerebral malaria in inbred mice. I. A new model and its pathology. Trans R Soc Trop Med Hyg 1982, 76:410–415
13. Thumwood CM, Hunt NH, Clark IA, Cowden WB: Breakdown of blood-brain barrier in murine cerebral malaria. Parasitology 1988, 96:570–589
14. Neill AL, Hunt NH: Pathology of fatal and resolving *Plasmodium berghei* cerebral malaria in mice. Parasitology 1992, 195:165–175
15. Grau GE, Piguet PF, Engers Howard D, Louis JA, Vassalli P, Lambert PH: L3T4$^+$ T lymphocytes play a major role in the pathogenesis of murine cerebral malaria. J Immunol 1986, 137:1348–2354
16. Chan-Ling T, Neil AL, Hunt NH: Early microvascular changes in murine cerebral malaria detected in retinal wholemounts. Am J Pathol 1992, 140:1121–1129
17. Neill AL, Chan-Ling T, Hunt NH: Comparisons between microvascular changes in cerebral and non-cerebral malaria in mice, using the retinal wholemount technique. Parasitology 1993, 107:477–487
18. Thumwood CM, Hunt NH, Cowden WB, Clark IA: Antioxidants can prevent cerebral malaria in *Plasmodium berghei*-infected mice. Br J Exp Pathol 1989, 70:293–303
19. Lewallen S, Taylor TE, Molymeux ME, Wills BA, Courtright P: Ocular fundus findings in Malawian children with cerebral malaria. Ophthalmology 1993, 100: 857–861
20. Hidayat AA, Nalbandian RM, Sammons DW, Fleischman JA, Johnson TE: The diagnostic histopathological features of ocular malaria. Ophthalmology 1993, 100:1183–1186
21. Looareesuwan S, Warrell DA, White NJ, Chanthavanich P, Warrell MJ, Chantaratherakitti S, Changswek S, Chongmankongcheep L, Kanchanaranya C: Retinal hemorrhage, a common sign of prognostic significance in cerebral malaria. Am J Trop Med Hyg 1983, 32:911–915
22. Grau GE, Fajardo L, Piguet PF, Allet B, Lambert PH, Vassalli P: Tumor necrosis factor (cachectin) as an essential mediator in murine cerebral malaria. Science 1987, 237:1210–1212
23. de Kossodo S, Grau GE: Role of cytokines and adhesion molecules in malaria immunopathology. Stem Cells 1993, 11:41–48
24. Ockenhouse CF, Ho M, Tandon NN, Van Seventer GA, Shaw S, White NJ, Jamieson GA, Chulay JD, Webster HK: Molecular basis of sequestration in severe and uncomplicated *Plasmodium falciparum* malaria: differential adhesion of infected erythrocytes to CD36 and ICAM-1. J Infect Dis 1991, 164:163–169
25. Ockenhouse CF, Tegoshi T, Maeno Y, Benjamin C, Ho M, Kan KE, Thway Y, Win K, Aikawa M, Lobb RR: Human vascular endothelial cell adhesion receptors for *Plasmodium falciparum*-infected erythrocytes: roles for endothelial leukocyte adhesion molecule 1 and vascular cell adhesion molecule 1. J Exp Med 1992, 176: 1183–1189
26. Turner GDH, Morrison H, Jones M, Davis TM, Looareesuwan S, Buley ID, Gatter KC, Newbold CI, Pukritayakamee S, Nagachinta B, White NJ, Berendt AR: An immunohistochemical study of the pathology of fatal malaria: evidence for widespread endothelial activation and a potential role for intercellular adhesion molecule-1 in cerebral sequestration. Am J Pathol 1994, 145:1057–1069
27. Bevilacqua MP: Endothelial-leukocyte adhesion molecules. Annu Rev Immunol 1993, 11:767–804
28. Jakobsen PH, Morris-Jones S, Rønn A, Hviid L, Theander TG, Elhassan IM, Bygbjerg IC, Greenwood BM: Increased plasma concentrations of sICAM-1, sVCAM-1 in patients with *Plasmodium falciparum* or *P. vivax* malaria and association with disease severity. Immunology 1994, 83:665–669
29. Wenisch C, Varijsnonta S, Looareesuwan S, Graninger W, Pichler R, Wernsdorfer W: Soluble intercellular adhesion molecule-1 (ICAM-1), endothelial leukocyte adhesion molecule-1 (ELAM-1), and tumor necrosis factor receptor (55 kDa TNF-R) in patients with acute *Plasmodium falciparum* malaria. Clin Immunol Immunopathol 1994, 71:344–348
30. Chan-Ling T: A method for studying glial, vascular and neuronal cytogenesis in wholemount cat retina. Res Micro Tech (in press)
31. Chan-Ling T, Tout T, Holländer H, Stone J: Vascular changes and their mechanisms in the feline model of retinopathy of prematurity. Invest Ophthalmol Vis Sci 1992, 33:2128–2147
32. McKinney MM, Parkinson A: A simple, non-chromatographic procedure to purify immunoglobulins from serum and ascites fluid. J Immunol Methods 1987, 96: 271–278
33. Prieto J, Takei F, Gendelman R, Christenson B, Biberfeld P, Patarroyo M: MALA-2, mouse homologue of human adhesion molecule ICAM-1 (CD54). Eur J Immunol 1989, 19:1551–1557
34. Medana IM, Chan-Ling T, Hunt NH: Redistribution and degeneration of retinal astrocytes in experimental murine cerebral malaria: relationship to disruption of the blood-retinal barrier. Glia 1996, 16:51–64
35. Holländer H, Makarov F, Dreher Z, Driel DV, Chan-Ling T, Stone J: Structure of the macroglia of the retina: sharing and division of labour between astrocyte and Müller cells. J Comp Neurol 1991, 313:587–603
36. Stewart PA, Tuor UI: Blood-eye barrier in the rat: correlation of ultrastructure with function. J Comp Neurol 1994, 340:566–576
37. Schofield L, Novakovic S, Gerold P, Schwarz RT, McConville MJ, Tachado SD: Glycosylphosphatidyli-

nositol toxin of *Plasmodium* upregulates intercellular adhesion molecule-1, vascular cell adhesion molecule-1, and E-selectin expression in vascular endothelial cells and increases leukocyte and parasite cytoadherence via tyrosine kinase-dependent signal transduction. J Immunol 1996, 156:1886–1896

38. Ghigo D, Todde R, Ginsburg H, Costamagna C, Gautret P, Bussolino F, Ulliers D, Giribaldi G, Deharo E, Gabrielli G: Erythrocyte stages of *Plasmodium falciparum* exhibit a high nitric oxide synthase (NOS) activity and release an NOS-inducing soluble factor. J Exp Med 1995, 182:677–688
39. Greenwood J: Mechanisms of blood-brain barrier breakdown. Neuroradiology 1991, 33:95–100
40. Grau GE, Piguet P-F, Vassalli P, Lambert P-H: Tumor-necrosis factor and other cytokines in cerebral malaria: experimental and clinical data. Immunol Rev 1989, 112:49–70
41. Neill AL, Hunt NH: Effect of endotoxin and dexamethasone on cerebral malaria in mice. Parasitology 1995, 111:443–454
42. Claudio L, Martiney JA, Brosnan CF: Ultrastructural studies of the blood-retina barrier after exposure to interleukin-1β or tumor necrosis factor-α. Lab Invest 1994, 70:850–861
43. Hunt NH, Manduci N, Thumwood CM: Amelioration of murine cerebral malaria by dietary restriction. Parasitology 1993, 107:471–476
44. Clark IA, Ilschner S, MacMicking JD, Cowden WB: TNF and *Plasmodium berghei* ANKA-induced cerebral malaria. Immunol Lett 1990, 25:195–198
45. Fabry Z, Waldschmidt MM, Hendrickson D, Keiner J, Love-Homan L, Takei F, Hart MN: Adhesion molecules on murine brain microvascular endothelial cells: expression and regulation of ICAM-1 and Lgp 55. J Neuroimmunol 1992, 36:1–11
46. MacPherson GG, Warrell MJ, White NJ, Looareesuwan S, Warrell DA: Human cerebral malaria: a quantitative ultrastructural analysis of parasitized erythrocyte sequestration. Am J Pathol 1985, 119:385–401
47. Grau GE, Pointaire P, Piguet P-F, Vesin C, Rosen H, Stamenkovic I, Takei F, Vassalli P: Late administration of monoclonal antibody to leukocyte function-antigen 1 abrogates incipent murine cerebral malaria. Eur J Immunol 1991, 21:2265–2267
48. Falanga PB, Butcher EC: Late treatment with anti-LAF-1 (CD11a) antibody prevents cerebral malaria in a mouse model. Eur J Immunol 1991, 21:2259–2263
49. Grau GE, Tacchini-Cottier F, Vesin C, Milon G, Lou JN, Piguet P-F, Juillard P: TNF-induced microvascular pathology: active role for platelets and importance of the LFA-1/ICAM-1 interaction. Eur Cytokine Network 1993, 4:415–419
50. Bate CAW, Roman TE, Moreno C, Playfair JHL: Tumor necrosis factor induction by malaria exoantigens depends upon phospholipid. Immunology 1992, 75:129–135
51. Tachado SD, Schofield L: Glycosylphosphatidylinositol toxin of *Trypanosoma brucei* regulates IL-1α and TNF-α expression in macrophages by protein tyrosine kinase mediated signal transduction. Biochem Biophys Res Commun 1994, 205:984–991